Feist, F., Menzel, J. P., Weil, T., Blinco, J., & Barner-Kowollik, C. (2018). Visible Light-Induced Ligation via o-Quinodimethane Thioethers. Journal of the American Chemical Society, 140(37), 11848-11854. doi:10.1021/jacs.8b08343.

Visible Light-Induced Ligation via o-Quinodimethane Thioethers

Feist, F., Menzel, J. P., Weil, T., Blinco, J., & Barner-Kowollik, C.

Visible Light Induced Ligation *via o*-Quinodimethane Thioethers

Florian Feist,[†§] Jan P. Menzel,[†] Tanja Weil,*[§] James P. Blinco*[†] and Christopher Barner-Kowollik*[†‡]

[†] *School of Chemistry, Physics and Mechanical Engineering, Queensland University of Technology (QUT), 2 George Street, Brisbane, QLD 4000, Australia*

[§] *Max Planck Institute for Polymer Research, Ackermannweg 10, 55128 Mainz, Germany*

[‡] *Macromolecular Architectures, Institut für Technische Chemie und Polymerchemie, Karlsruhe Institute of Technology (KIT), Engesserstr. 18, 76131 Karlsruhe, Germany*

Supporting Information Placeholder

ABSTRACT: We introduce a photocaged diene system (*o*-quinodimethane thioethers) based on *o*-methylbenzaldehydes (*o*-MBAs) that can be activated with visible light. The pioneered system is accessible in a single step from commercially available starting materials in excellent yields. Variable synthetic handles can be attached to the photocaged diene, often without elaborate protecting group chemistry. Full conversion of various *o*-methylbenzaldehydes to the Diels-Alder adduct is achieved in the presence of maleimides under catalyst free conditions triggered by visible light irradiation with LEDs under flow conditions. Unlike the previously reported UV-induced ligation of *o*-quinodimethanes, the reaction can be conducted both in organic solvents and aqueous solution. We further demonstrate the ability of the photo-caged dienes to ligate two polymer blocks by visible light. The [4+2] nature of the reaction makes it a powerful orthogonal ligation platform.

INTRODUCTION

The click chemistry concept introduced by Kolb, Finn and Sharpless, has emerged as a pivotal tool in contemporary small molecule synthesis as well as polymer chemistry. The concept focuses on function and properties rather than on complex multi-step synthesis.[1] The hypothesis that functional molecules can be obtained by combining molecular building blocks with highly efficient ligation reactions has been amply demonstrated in the following years in countless studies, especially in the field of bio-[2] and polymer chemistry.[3,4] Light induced click reactions critically enhance the concept with spatio-temporal control.[5] In contrast to reactions requiring a catalyst, for instance the photochemical reduction of Cu(II) to Cu(I) catalysing a copper-mediated azid alkyne coupling (CuAAC),[6] photo-click reactions only involve two substrates allowing for the highest possible control over the reaction. Photochemical patterned surface functionalization,[7] conjugation of biomolecules[8] and macromolecules, 3D stereolithography,[9-10] light induced folding of single-chain nanoparticles,[11-12] as well as reactions in living cells[2] are among the various applications of such reactions. Bioorthogonal ligations require an exceptional level of efficiency and chemical selectivity resulting in minimal interference with existing biological components. Reactions that perform well *in vivo* can therefore be considered the gold-standard of click reactions.[13-14] Especially the photochemically controlled strain-promoted azide alkyne coupling (photo-SPAAC) and the 1,3-dipolar cycloaddition between a nitrile imine generated from a tetrazole under light irradiation and an alkene (Nitrile Imine mediated Tetrazole Ene Cycloaddition,

NITEC) are both often considered to be bioorthogonal.[2, 15-16] However, despite their asserted bioorthogonality, specific limitations apply when these reactions are employed. For example, nitrile imines react with various functional groups (including amines, thiols, carboxylic acids and heterocycles) limiting their chemical selectivity.[17] Thus, the development of reactions with exceptional selectivity and mild trigger wavelength remains critically important. To date, the majority of the established photoinduced ligation reactions require UV light. For several applications such as coupling of photosensitive entities or chemistry in living cells, the use of UV-light constitutes a formidable barrier.[18] Shifting the absorption and reactivity of photoreactive molecules into the visible range while preserving orthogonality and biocompatibility, though avoiding potentially toxic transition metal catalysts, constitutes a key aim in contemporary photochemistry.[19-21]

Despite considerable research efforts, only few of the known efficient UV-photoligations have been adapted for visible light activation. For example, the NITEC reaction was shifted to 405 nm by the attachment of a terthiophene unit to the 2-position of the tetrazole.[18, 22]
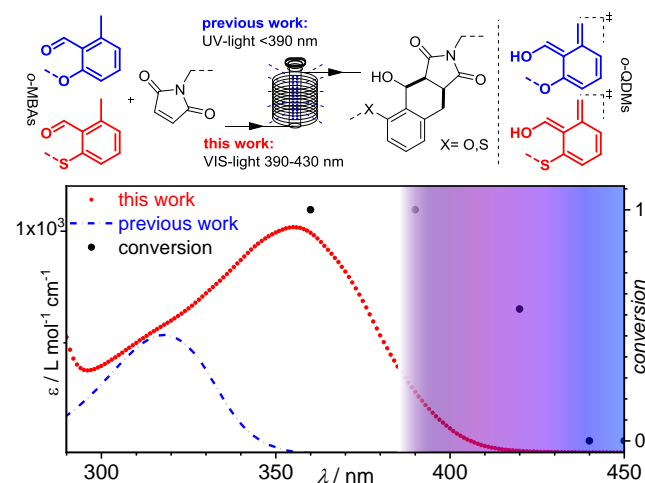
Scheme 1: (Top) Structural overview of the red-shifted *o*-QDMs of the current study (red) and the most recent state-of-the-art *o*-QDMs (blue). In the present study, transformations are carried out in photoflow. (Bottom) Red-shifted UV-VIS absorption spectrum of *o*-MBAs and wavelength-resolved fractional conversion using a tunable laser and constant photon count (30 µmol, for details refer to the Supporting Information section 1.9), shown on the example of species **A1** (see Scheme 2) recorded in DCM. The visible range of the spectrum is depicted using the RGB-equivalents of the corresponding wavelength.

The use of conjugated π-systems to shift the absorption and reactivity from the UV to the visible-region was successfully demonstrated in azirines, acylsulfides and styryl-compounds.[23-25]

The photochemically induced generation of reactive dienes, for instance *o*-QDMs or naphtoquinon-3-methides (*o*-MQMs)[15,26] and their subsequent (hetero)-Diels-Alder reaction with electron deficient enes is one of the most important strategy for photoclick ligations. These find wide-spread applications in, for example, the synthesis of sequence-defined macromolecules,[27] single-chain folding,[28-30] surface functionalization,[31] light-induced assembly of nanostructures,[32] and photoresists for 3D direct laser writing.[9-10] Recently, the wavelength-dependency of *o*-QDMs formed from an *o*-methyl benzaldehyde (*o*-MBA) and its subsequent Dieles-Alder reaction was explored in detail. Underpinned by time-dependent density functional theory (TD-DFT) calculations this investigation allowed for an in-depth understanding of the mechanism and photo-physical properties of the reaction.[33] A large number of synthetically valuable transformations including light-induced reactions based on *o*-QDMs have been reported,[34] including various organocatalytic strategies to for enantioselective trapping of *o*-QDMs.[35] Especially the generation of hetero aza-*o*-xylylenes (heteroatom analogue *o*-QDMs) was repeatedly used to enable elegant syntheses of complex structural motifs.[36-39] To the best of our knowledge, there is only one report that indicates the formation of *o*-QDMs using visible light: Furukawa and coworkers reported in 1993 that 8,13-dihydrobenzo[*g*]naphtho[1,8-*bc*][1,5]di-selenonine form *o*-QDMs under exposure of ambient laboratory light.[40] This interesting reaction forms naphtho[1,8-*cd*][1,2]diselenole in stoichiometric quantities, thus requiring chromatographic purification. Critically, it involves toxic organoselenium compounds and can thus not be considered a viable (bio)-ligation strategy.

The current contribution provides a simple to access visible light induced [4+2] ligation technology platform, shifting the wavelength of activation well into the visible light regime up to 430 nm via a simple oxygen/sulfur exchange within the *o*-MBA's structure (refer to Scheme 1).

RESULTS and DISCUSSION
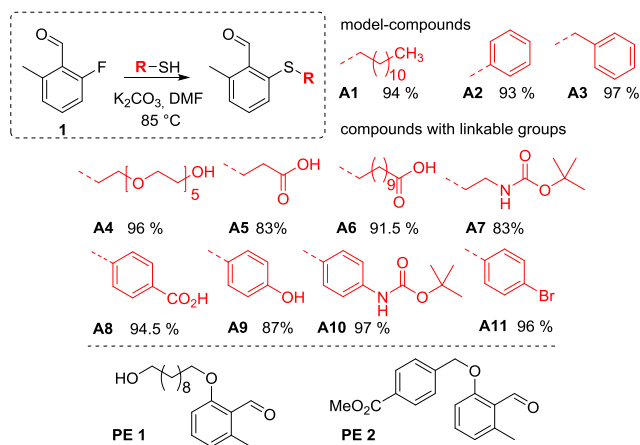
Scheme 2: (Top) Synthesis and isolated yields of red-shifted *o*-MBAs **A1-A3** and various other herein prepared *o*-MBAs with attached linker groups by reaction of 2-fluoro-6-methyl benzaldehyde **1** with the respective thiol. (Bottom) Structures of literature reported state-of-the-art *o*-MBAs **PE 1** (2-((10-hydroxydecyl)oxy)-6-methylbenzaldehyde) and **PE 2** PE 2 methyl (4-((2-Formyl-3-methylphenoxy)methyl)benzoate).[31, 41]

To activate a photoreactive compound with visible light, the molecule must possess two key properties. First, visible light must be absorbed and a reactive intermediate with a lifetime suitable for a chemical reaction must be formed. Second, the photochemically generated intermediate needs to selectively react with the target substrate. Here, we address these requirements by simply replacing oxygen with sulfur (Scheme 1), lowering the energy gap for the π-π* transition that leads to the formation of *o*-QDMs. In addition to the red-shift in absorption, the thioether moiety might also enforce a favourable conformation to enable the excited-state intramolecular proton transfer (ESIPT)[37, 39] that takes place during *o*-QDM formation. Such an *ortho*-effect was for instance studied in detail for the Bergman-cyclisation.[42] Furthermore, the n-donor properties of the thioether group might contribute to the nucleophilicity of the formed *o*-QDMs enabling an efficient Diels-Alder cycloaddtion with electron deficient enes.

The synthesis of non-functionalized model *o*-MBAs and *o*-MBAs functionalized with linker groups was achieved via literature adapted one-step procedure from commercially available 2-fluoro-6-methylbenzaldehyde **1**.[43] The optimization of the reaction conditions suggests that 85 °C and 12 h reaction time leads to full conversion in all cases indicated by the absence of ¹⁹F-NMR resonances. The desired products were obtained in excellent isolated yields of 83-97 % (for detailed analytical information refer to the Supporting Information section, Figs. S4-S25). The synthetic strategy represents a considerable advantage over previously reported functional *o*-MBAs that are only accessible in a 3-step procedure for hydroxyl-terminated systems and a 4-step procedure for carboxy-terminated variants with low yields (25 and 14%, respectively).[31, 41] Critically, compared to other visible light photosystems that often require laborious synthesis especially when chromophores are attached to the photoreactive entity, the herein established synthesis is simple and versatile.[18, 23-25]

The UV-vis absorption spectra of the three model-compounds **A1**, **A2**, and **A3**, depicted in supporting Fig. S64 indicate an π-π* transition absorption maximum between

350-360 nm tailing into the visible region (refer to the zoom between 390-450 nm). Compared to the previously reported o-MBAs **PE1** and **PE2**[31, 41] (Scheme 2, Fig S64, SI) featuring an π-π* transition at approximately 320 nm, our new compounds are red-shifted by close to 40 nm in their absorption. Aryl-aryl thioether **A2** shows the strongest tailing into the visible region. In an action plot, the conversion of a photoreactive molecule is probed at a constant photon count at different monochromatic wavelengths. For the o-MBA UV-only active **PE2**, Menzel et al.[33] recorded an action plot, demonstrating that the compound still shows some very limited photoreactivity up to 390 nm. Assuming the new red-shifted compounds show a similar wavelength-dependent behaviour, we expected that the new compounds would be reactive under visible light irradiation. Since the structure of the transient o-QDM is rather similar to the previously reported molecule **PE2**, we envisaged that trapping with a suitable dienophile would be comparably efficient. We thus herein assess the photoligation of model-compounds **A1**, **A2** and **A3** by trapping their transient o-QDM species with dienophile **B1** at λ_{max}= 410 nm (LED, emission spectra shown in the SI, Figure S1) in a photoflow reactor with a retention

time of 10 min at 20 °C. Alkyl-arylthiother **A1** was quantitatively converted to product **C1** in the presence of dienophile **B1** and Aryl-aryl thioether **A2** also quantitatively afforded the cycloadduct **C2** under identical conditions (Figure 1, for additional spectroscopic data refer to the Supporting Information Figs. S28 to S29). Note that the spectra shown in Figure 1 were obtained without any purification and result exclusively from merely removing the solvent. However, benzyl-arylthioether **A3** did not react selectively to the desired cycloadduct **C3**. Thus, the NMR-spectra after irradiation of **A3** in presence of **B1** show not only the new resonances for the cycloadduct **C3** but also new signals between 10 and 11 ppm. We assume that either α-cleavage or α-H abstraction takes place along with the desired cycloaddition. Critically, **A1** and **A2** were also quantitatively converted to cycloadducts **C1** and **C2** using a λ_{max}= 430 nm LED, albeit with a longer retention time of 20 min (emission spectra of the LEDs and overlay with UV-vis spectra of o-MBAs **A1-A3**, SI Fig. S65). The NMR spectra after irradiation at 365 nm, and 430 nm – again without any further purification – are depicted in supporting Figures Figs. S45-S46.
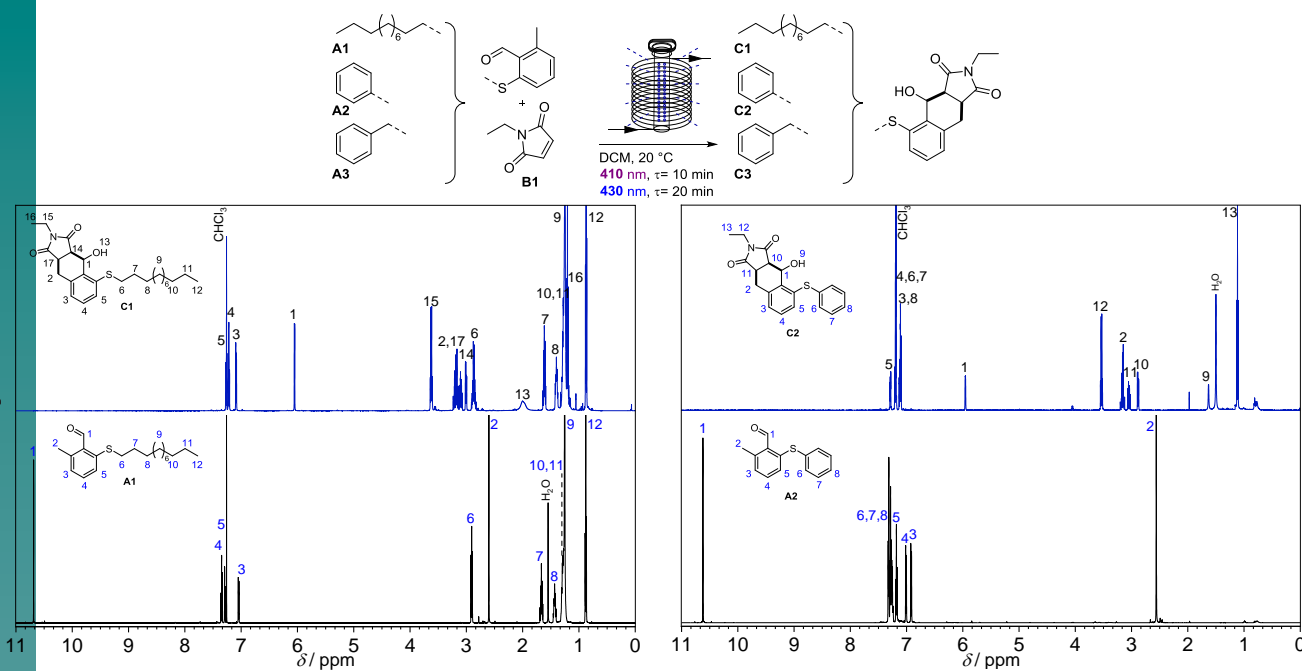

Figure 1 (Top) Reaction between o-MBAs **A1-A3** and **B1** to form cycloadducts **C1-C3** under visible light irradiation (LED-emission spectra refer to supporting Figs. S1). (Bottom) ¹H-NMR spectra obtained of **A1, C1, A2, C2** with assigned resonances. No purification was carried out for **C1** and **C2**, indicating the extremely high selectivity of the photoligation. **A3** forms non-selective products with **B1**. Detailed analytical information for all compounds depicted in Fig. 1 can be found in the supporting Figs. S4-S9 and S26-S29.
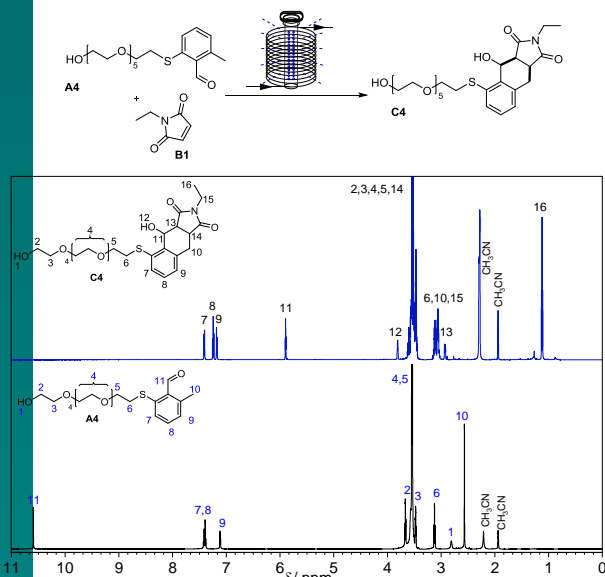
Figure 2: (Top) Photoligation of **A4** and **B1** in acetonitrile to form cycloadduct **C4**, ^{1}H-NMR spectrum of **A4** (bottom) and the photoproduct **C4** (middle). Detailed analytical information for all compounds depicted in Fig. 2 can be found in the supporting Figs. S10-S11, S30-S31 and S54-S55

In addition to the photoflow experiments, batch-experiments with a tunable laser, in order to precisely determine the maximum wavelength for visible light activation of substrate **A1** were performed. This was achieved through irradiation of samples at 360, 390, 420, 440 and 450 nm with the same number of photons in deuterated acetonitrile (ACN) with equimolar stoichiometry. The conversion was determined *via* ^{1}H-NMR. The resulting wavelength-resolved action plot is included in Scheme 1 above (for the detailed NMR spectra refer to the Supporting Information Fig. S44).

To examine the performance of the reaction at different wavelengths, retention times and solvents, we performed experiments using substrate **A4** as it ionizes well during ESI mass spectrometry and is therefore ideal for additional LC-MS analysis. In addition, **A4** is soluble in most common solvents. Cycloadduct **C4** was obtained in high purity without any purification on the preparative scale after irradiation of **A4** in the presence of a slight excess (1.10 eq.) of **B1** with 410 nm in acetonitrile after a flow retention time of 20 min (refer to Figure 2).

The results for the flow-experiments of **A4** and **B1** are collated in Table 1. The corresponding ^{1}H-NMR-spectra, LC-MS traces and mass spectra can be found in the Supporting Information section (Figs. S 10-11, 30-31, 47-51, 54-55, 59-61). For acetonitrile and toluene, we observed product formation with the highest selectivity towards **C4** , including its potentially formed stereoisomers. Stereoisomerism leads to more complex NMR and LC-MS spectra, although for a ligation technique the stereochemistry of the formed link is not critical under most circumstances. We additionally investigated the ligation in DMF and DMSO, where the previously reported *o*-MBAs[31, 41] performed very poorly, limiting the substrate scope for photoinduced ligations considerably. In contrast, we observed ligation, while the perfect endo-selectivity found in dichloromethane (Figure 1), acetonitrile and toluene (Table 1) was reduced in DMF. We identified a minor side-product (not exceeding 10% in the worst case) in less favorable solvents such as DMF and DMSO formed by oxidation, consuming the residual oxygen in the reaction

solution after deoxygenation by saturation with N_2. Identification of *ox*-**A4** was possible by comparing NMR and LC-MS spectra of a purposeful synthesized *ox*-**A4** by oxidation of **A4** with sodium periodate in EtOH/H_2O. The analytical data for *ox*-**A4** is given in Figs. S38-39 and S58 in the Supporting Information.
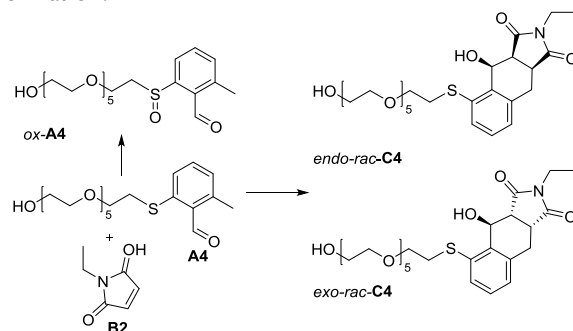
Scheme 3: Main ligation products *endo-rac*-C4 and *exo-rac*-C4 as well as minor side-product identified during the photoinduced Diels-Alder reaction of **A4** and **B1** in DMF and DMSO.

Table 1: Flow photoligation experiments using **A4** and **B1** in different solvents. LED-irradiation wavelengths (λ_{max}), retention time (τ), X^a conversion evaluated via ^{1}H-NMR (based on the aldehyde-resonance numbered 11 within the starting material vs. the α-hydroxy-resonance 11 of the product, refer to Fig. 2). X^b conversion evaluated via LC-MS (UV-detection at 254 nm). *endo-rac*-**C4**/*exo-rac*-**C4** ratio of the endo and exo-cycloadduct depicted in **Scheme 3**.

Solvent	λ_{max} [nm]	τ [min]	X^a [%]	X^b [%]	endo-rac-**C4**/ exo-rac-**C4**	ox-A4 [%]
ACN	365	10	98	98	>99:1	<1
	410	10	96	95	>99:1	0
	410	20	100	100	>99:1	0
	430	10	60	61	>99:1	0
	430	20	98	97	>99:1	0
Toluene	365	10	100	97	>99:1	0
	410	10	99	99	>99:1	0
	430	10	80	79	>99:1	0
	430	20	100	99	>99:1	0
DMF	365	10	81	78	76:24	2
	365	20	85	-	75:25	3
	410	10	35	33	80:20	1
	410	20	63	58	65:35	8
	410	30	84	-	65:35	2
	430	20	19	17	70:30	1
	430	40	36	-	67:23	2
DMSO	365	10	43	-	>99:1	3
	365	20	48	-	>99:1	7
	410	20	47	-	>99:1	1
	430	20	28	-	>99:1	10

4

One of the key attractive features of our new class of visible light reactive *o*-MBAs is the ability to conduct the photoligation in aqueous media, which opens considerable avenues for bioorthogonal ligation. In Fig. 3, the reaction between the water soluble 'hexaethylene glycol-*o*-MBA' **A4** and the water soluble 'hexaethylene glycol-maleimide' **B2** under flow conditions and irradiation with UV and visible light is explored. Surprisingly, the new red-shifted *o*-MBA reacts well in a mixture of 0.1 M PBS/water 50:50 *v/v*, typically used in bioligations. ¹H-NMR and LC-MS indicate close to quantitative conversion and selectivity using equimolar amounts of the starting materials.
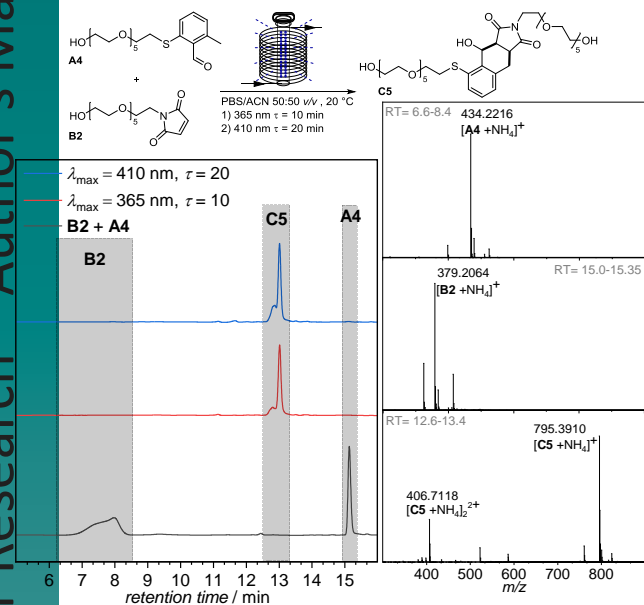

Figure 3: (Top) Aqueous photoinduced ligation between **A4** and **B2** affording cycloadduct **C4** at 365 and 410 nm (λ_{max}) in in a continuous flow reactor with 10 and 20 min retention time, respectively. (Bottom, left) LC-traces (UV-detection at 215 nm). Note that **B2** elutes broadly under the elution conditions required for optimized product elution. (Bottom, right) Accumulated mass spectra from the LC-traces with the accumulated area marked in grey and annotated masses for the most abundant ions. Detailed analysis of the mass spectra and ¹H-NMR can be found in Supporting Information Figs. S52 and S56.

In a subsequent step, we explored the reactivity of our red-shifted *o*-MBAs towards alternative dienophiles. Of particular interest are those that also constitute mediating agents for reversible deactivation radical polymerization (RDRP). A particularly attractive reagent is cyanoisopropyldithiobenzoate (CPDB, **B3**), which is a versatile controlling entity for a wide monomer range during reversible addition fragmentation chain transfer (RAFT) polymerization.[44-45] **B3** was converted to cycloadduct **C6** in ACN under equimolar conditions with visible light irradiation at 410 nm at a retention time of 20 min. Figure 4 shows the LC-MS traces of **A4** and **C6** as well as the associated high resolution mass spectra, attesting the efficiency of the phototransformation (isolated yield 91%, refer to the Supporting Information for an in-depth discussion of the associated spectra, Figs. S32-33, S57). Ligation at 410 nm is a critical improvement over the current state-of-the-art reported by Oehlenschlaeger *et al.*, who employed 320 nm (λ_{max}) to afford the cycloadduct.[46]

Given that **B3** is a RAFT agent, it is mandatory to assess the visible light ligation of two disparate polymer blocks present in equimolar ratios (end groups) in flow. We thus prepared

P1, a poly(ε-caprolactone) carrying our red-shifted *o*-MBA structure, and **P2**, a poly(methyl methacrylate). Figures 5 illustrates the size exclusion chromatography (SEC) traces of **P1** and **P2** as well as the ligation product **P1-P2**, clearly evidencing the formation of the block copolymer structure at higher elution volumes. Note that the ring opening process employed for the formation of **P1** limits the initial dispersity of the starting polymer.
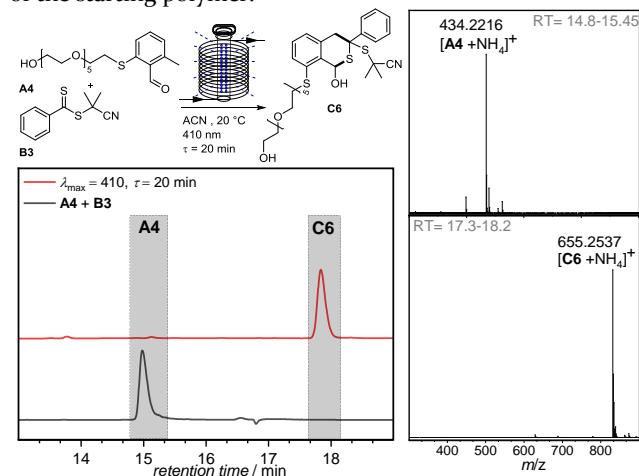

Figure 4: (Top, left) Reaction scheme of *o*-MBA **A4** and dithioester **B3** forming cycloadduct **C6**. (Right) UV-detector traces (254 nm detection wavelength) of **A4** and **C6**, respectively.

Additionally shown in Figure 5 are the UV/Vis spectra of **P1** and **P1-P2**, clearly reveal that the n-π* transition associated with the thiocarbonlythio chain terminus of **P2** disappears, leading to a non-colored reaction product. The ability of our red-shifted *o*-MBAs to ligate polymer chains demonstrate the applicability of our system for complex polymer construction.
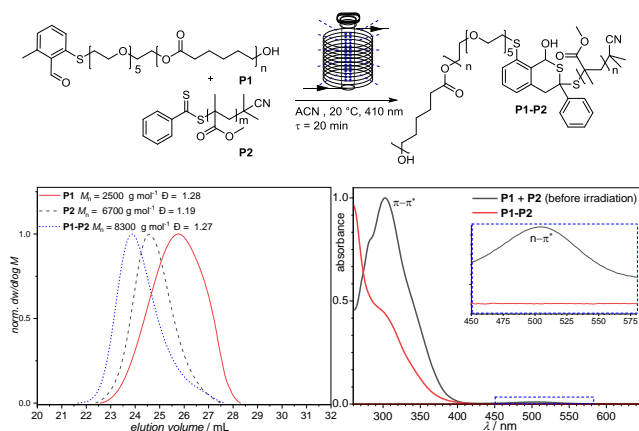

Figure 5: (Top) Visible-light induced ligation of *o*-MBA-ROP-polymer P1 and RAFT-polymer P2 to form P1-P2 and (bottom, left) THF-SEC-results. (Bottom, right) UV-vis spectra of P1 and P1-P2 recorded ACN. For NMR, SEC and SEC-ESI MS refer to the Supporting Information Figs. S42-43 and S62-63 as well as Table S9

CONCLUSIONS

We introduce a new synthetic platform for visible-light induced [4+2] ligation based on ready-to-access *o*-MBAs (photocaged *o*-QDMs) with electron deficient enes. The visible light *o*-MBAs are readily prepared and feature efficient photoactivation under visible-light irradiation up to 430 nm. The visible light activation was independently mapped (action

plot) using a monochromatic laser light source in batch-experiments. Critically, we demonstrate that o-QDM ligation proceeds quantitatively in aqueous environments, which is important for its applicability in bioligations. Further, we demonstrate the visible light [4+2] ligation in various solvents including ACN, toluene, dichloromethane (DCM) as the most suitable systems, while DMSO and DMF allow the reaction to proceed, albeit at lower reaction rates. Finally, the visible light activation of o-MBA-thioethers was employed for the ligation of two disparate polymer strands. The herein introduced new class of visible light photochemical ligation agents thus represents a simple to access, versatile and efficient tool for diverse synthetic scenarios. In addition, red-shifted catalyst-free ligation is essential for establishing λ-orthogonal reaction systems[47-48] required for multi-material 3D laser lithography.[49]

ASSOCIATED CONTENT

Supporting Information

Materials, Instrumentation, Synthetic procedures, Supporting Spectroscopic Data. The Supporting Information is available free of charge on the ACS Publications website.

AUTHOR INFORMATION

Corresponding Authors

weil@mpip-mainz.mpg.de

j.blinco@qut.edu.au

christopher.barnerkowollik@qut.edu.au,

christopher.barner-kowollik@kit.edu

Notes

The authors declare no competing financial interests.

ACKNOWLEDGMENT

REFERENCES

(1)   Kolb, H. C.; Finn, M. G.; Sharpless, B. G., *Angew. Chem. Int. Ed.* **2001**, *40*, 2004-2021.

(2)   Lim, R. K. V.; Lin, Q., *Acc. Chem. Res.* **2011**, *44* (9), 828-839.

(3)   Espeel, P.; Du Prez, F. E., *Macromolecules* **2014**, *48* (1), 2-14.

(4)   Patterson, D. M.; Nazarova, L. A.; Prescher, J. A., *ACS Chem. Biol.* **2014**, *9* (3), 592-605.

(5)   Tasdelen, M. A.; Yagci, Y., *Angew. Chem. Int. Ed.* **2013**, *52* (23), 5930-8.

(6)   Castro-Godoy, W. D.; Heredia, A. A.; Schmidt, L. C.; Argüello, J. E., *RSC Advances* **2017**, *7* (54), 33967-33973.

(7)   Delaittre, G.; Goldmann, A. S.; Mueller, J. O.; Barner-Kowollik, C., *Angew. Chem. Int. Ed.* **2015**, *54* (39), 11388-403.

(8)   Wang, J.; Zhang, W.; Song, W.; Wang, Y.; Yu, Z.; Li, J.; Wu, M.; Wang, L.; Zang, J.; Lin, Q., *J. Am. Chem. Soc.* **2010**, *132* (42), 14812-14818.

(9)   Quick, A. S.; Rothfuss, H.; Welle, A.; Richter, B.; Fischer, J.; Wegener, M.; Barner-Kowollik, C., *Adv. Funct. Mater.* **2014**, *24* (23), 3571-3580.

(10)   Mueller, P.; Zieger, M. M.; Richter, B.; Quick, A. S.; Fischer, J.; Mueller, J. B.; Zhou, L.; Nienhaus, G. U.; Bastmeyer, M.; Barner-Kowollik, C.; Wegener, M., *ACS Nano* **2017**, *11* (6), 6396-6403.

(11)   Frisch, H.; Menzel, J. P.; Bloesser, F. R.; Marschner, D. E.; Mundsinger, K.; Barner-Kowollik, C., *J. Am. Chem. Soc.* **2018**, *140* (30), 9551-9557.

(12)   Hosono, N.; Gillissen, M. A. J.; Li, Y.; Sheiko, S. S.; Palmans, A. R. A.; Meijer, E. W., *J. Am. Chem. Soc.* **2013**, *135* (1), 501-510.

(13)   Shah, L.; Laughlin, S. T.; Carrico, I. S., *J. Am. Chem. Soc.* **2016**, *138* (16), 5186-5189.

(14)   Baskin, J. M.; Bertozzi, C. R., *QSAR Comb. Sci.* **2007**, *26* (11-12), 1211-1219.

(15)   Arumugam, S.; Popik, V. V., *J. Am. Chem. Soc.* **2011**, *133* (14), 5573-9.

(16)   Arumugam, S.; Popik, V. V., *J. Am. Chem. Soc.* **2012**, *134* (20), 8408-11.

(17)   Li, Z.; Qian, L.; Li, L.; Bernhammer, J. C.; Huynh, H. V.; Lee, J. S.; Yao, S. Q., *Angew. Chem. Int. Ed.* **2016**, *55* (6), 2002-6.

(18)   An, P.; Yu, Z.; Lin, Q., *Chem. Commun.* **2013**, *49* (85), 9920-2.

(19)   Bleger, D.; Hecht, S., *Angew. Chem. Int. Ed.* **2015**, *54* (39), 11338-49.

(20)   Hemmer, J. R.; Poelma, S. O.; Treat, N.; Page, Z. A.; Dolinski, N.; Diaz, Y. J.; Tomlinson, W.; Clark, K. D.; Hooper, J. P.; Hawker, C. J.; Read de Alaniz, J., *J. Am. Chem. Soc.* **2016**, *138* (42), 13960-13966.

(21)   Yoon, T. P.; Ischay, M. A.; Du, J., *Nat. Chem.* **2010**, *2* (7), 527-32.

(22)   An, P.; Yu, Z.; Lin, Q., *Org. Lett.* **2013**, *15* (21), 5496–5499.

(23)   Tuten, B. T.; Menzel, J. P.; Pahnke, K.; Blinco, J. P.; Barner-Kowollik, C., *Chem. Commun.* **2017**, *53* (32), 4501-4504.

(24)   Mueller, J. O.; Schmidt, F. G.; Blinco, J. P.; Barner-Kowollik, C., *Angew. Chem. Int. Ed.* **2015**, *54* (35), 10284-10288.

(25)   Truong, V. X.; Li, F.; Ercole, F.; Forsythe, J. S., *ACS Macro Lett.* **2018**, *7* (4), 464-469.

(26)   Arumugam, S.; Popik, V. V., *J. Am. Chem. Soc.* **2009**, *131* (33), 11892-11899.

(27)   Zydziak, N.; Konrad, W.; Feist, F.; Afonin, S.; Weidner, S.; Barner-Kowollik, C., *Nat. Commun.* **2016**, *7*, 13672.

(28)   Altintas, O.; Willenbacher, J.; Wuest, K. N. R.; Oehlenschlaeger, K. K.; Krolla-Sidenstein, P.; Gliemann, H.; Barner-Kowollik, C., *Macromolecules* **2013**, *46* (20), 8092-8101.

(29)   Wedler-Jasinski, N.; Lueckerath, T.; Mutlu, H.; Goldmann, A. S.; Walther, A.; Stenzel, M. H.; Barner-Kowollik, C., *Chem. Commun.* **2017**, *53* (1), 157-160.

(30)   Blasco, E.; Tuten, B. T.; Frisch, H.; Lederer, A.; Barner-Kowollik, C., *Polymer Chemistry* **2017**, *8* (38), 5845-5851.

(31)   Pauloehrl, T.; Delaittre, G.; Winkler, V.; Welle, A.; Bruns, M.; Borner, H. G.; Greiner, A. M.; Bastmeyer, M.; Barner-Kowollik, C., *Angew. Chem. Int. Ed.* **2012**, *51* (4), 1071-4.

(32)   Chen, L.; Xu, M.; Hu, J.; Yan, Q., *Macromolecules* **2017**, *50* (11), 4276-4280.

(33)   Menzel, J. P.; Noble, B. B.; Lauer, A.; Coote, M. L.; Blinco, J. P.; Barner-Kowollik, C., *J. Am. Chem. Soc.* **2017**, *139* (44), 15812-15820.

(34)   Segura, J. L.; Martin, N., *Chem. Rev.* **1999**, *99*, 3199-3246.

(35)   Cuadros, S.; Melchiorre, P., *Eur. J. Org. Chem.* **2018**, *2018* (23), 2884-2891.

(36)   Mukhina, O. A.; Kuznetsov, D. M.; Cowger, T. M.; Kutateladze, A. G., *Angew. Chem. Int. Ed.* **2015**, *54* (39), 11516-11520.

(37)   Kuznetsov, D. M.; Mukhina, O. A.; Kutateladze, A. G., *Angew. Chem. Int. Ed.* **2016**, *55* (24), 6988-6991.

(38)   Kuznetsov, D. M.; Kutateladze, A. G., *J. Am. Chem. Soc.* **2017**, *139* (46), 16584-16590.

(39)   Mukhina, O. A.; Kutateladze, A. G., *J. Am. Chem. Soc.* **2016**, *138* (7), 2110-2113.

(40)   Fujihara, H.; Yabe, M.; Furukawa, N., *J. Org. Chem.* **1993**, *58* (20), 5291-5292.

(41)   Gruendling, T.; Oehlenschlaeger, K. K.; Frick, E.; Glassner, M.; Schmid, C.; Barner-Kowollik, C., *Macromol. Rapid Commun.* **2011**, *32* (11), 807-12.

(42)   Zeidan, T. A.; Kovalenko, S. V.; Manoharan, M.; Alabugin, I. V., *J. Org. Chem.* **2006**, *71* (3), 962-975.

(43)   Zhang, H. Q.; Xia, Z.; Kolasa, T.; Dinges, J., *Tetrahedron Lett.* **2003**, *44* (48), 8661-8663.

(44)   Moad, G.; Rizzardo, E.; Thang, S. H., *Chem. Asian J.* **2013**, *8* (8), 1634-1644.

(45)   Semsarilar, M.; Perrier, S., *Nat. Chem.* **2010**, *2*, 811.

(46)   Oehlenschlaeger, K. K.; Mueller, J. O.; Heine, N. B.; Glassner, M.; Guimard, N. K.; Delaittre, G.; Schmidt, F. G.; Barner-Kowollik, C., *Angew. Chem. Int. Ed.* **2013**, *52* (2), 762-6.

(47)   Hiltebrandt, K.; Kaupp, M.; Molle, E.; Menzel, J. P.; Blinco, J. P.; Barner-Kowollik, C., *Chem. Commun.* **2016**, *52* (60), 9426-9.

(48)   Hansen, M. J.; Velema, W. A.; Lerch, M. M.; Szymanski, W.; Feringa, B. L., *Chem. Soc. Rev.* **2015**, *44* (11), 3358-3377.

(49)   Barner-Kowollik, C.; Bastmeyer, M.; Blasco, E.; Delaittre, G.; Müller, P.; Richter, B.; Wegener, M., *Angew. Chem. Int. Ed.* **2017**, *56* (50), 15828-15845.